Cement & Concrete Composites 32 (2010) 73–83

Contents lists available at ScienceDirect

Cement & Concrete Composites

journal homepage: www.elsevier.com/locate/cemconcomp

Dimensional and ice content changes of hardened concrete at different freezing and thawing temperatures

Björn Johannesson

Department of Civil Engineering, Building 118, Technical University of Denmark, 2800 Lyngby, Denmark

ARTICLE INFO

Article history:
Received 8 January 2009
Received in revised form 7 September 2009
Accepted 11 September 2009
Available online 18 September 2009

Keywords:
Frost damages
Freezing
Thawing
Durability
Ice content
Scanning calorimeter

ABSTRACT

Samples of concrete at different water-to-cement ratios and air contents subjected to freeze/thaw cycles with the lowest temperature at about −80 °C are investigated. By adopting a novel technique, a scanning calorimeter is used to obtain data from which the ice contents at different freeze temperatures can be calculated. The length change caused by temperature and ice content changes during test is measured by a separate experiment using the same types of freeze–thaw cycles as in the calorimetric tests. In this way it was possible to compare the amount of formed ice at different temperatures and the corresponding measured length changes. The development of cracks in the material structure was indicated by an ultra-sonic technique by measuring on the samples before and after the freeze–thaw tests. Further the air void structure was investigated using a microscopic technique in which air 'bubble' size distributions and the so-called spacing factor, indicating the mean distance between air bubbles, were measured. By analyzing the experimental result, it is concluded that damages occur in the temperature range of about −10 °C to −55 °C, when the air content is lower than about 4% of the total volume. For a totally water-saturated concrete, damages always occur independently of the use of entrained air or low water-to-cement ratios. It is, further, concluded that the length changes of these samples correspond to the calculated ice contents at different temperatures in a linear fashion.

1. Introduction

The freeze/thaw resistance of concrete is highly dependent of the amount of entrained air besides the mechanical strength. Natural occurring amounts of air in concrete, i.e., about 1–2% of total volume, have generally been shown to produce concrete not being frost durable. For this reason, concrete for outdoor climate in countries with cold winters is almost always supplied with air contents of about 4–6%, which in most cases give a good performing product.

Here results are presented on ice contents, measured using a calorimetric technique, at different freezing/thawing temperatures. An approximate method of evaluating the ice contents from the calorimetric data is presented. Length changes are measured on separate parallel samples exposed to identical freezing/thawing conditions as the samples tested in the calorimetric device. The results from this investigation can potentially be used to identify some of the hypotheses which have been proposed for the ice growth and ice induced damage of cement based materials.

Theoretical considerations, using the concepts behind the so-called 'hydraulic pressure', state that the distances between the entrained air voids are of crucial importance for the determination of the frost resistance. The background is that formed ice in the spatial domains surrounding air voids, having much smaller pores than the entrained air spaces, pushes water not yet being frozen away from where the ice is formed and eventually reaches an air filled void. The assumption is that this flow of water builds up a mechanical pressure which, among other things, is proportional to the ice formation rate. If the entrained air voids are too far apart, the theory predicts that the developed water flow pressures exceed the tensile strength of the material. The method relies on the fact that one assumes that the domains surrounding air voids are at such a high water saturation level that pressures and hence water flows can be induced [1,2]. Since the ice formation rate is central in the above-mentioned hypothesis, investigations have been performed on the influence of freezing temperature on the mechanical behaviour of concrete. Some investigations, however, show very little influence of the rate of freezing rate, e.g. see [3,4].

If the material is totally water saturated, meaning that also the air voids are water filled, the theory behind the hydraulic pressure is not applicable since water not yet being frozen cannot escape from where the ice is formed. In this case the 'closed container model' is instead valid, which simply calculates the stress induced by the volume increase of water due to the freeze process. Further, simple thermodynamic calculations, using the Clapeyron equation, yield a pressure increase of approximately 10 MPa/K for 'free'

E-mail address: bjo@byg.dtu.dk

0958-9465/$ - see front matter © 2009 Elsevier Ltd. All rights reserved.
doi:10.1016/j.cemconcomp.2009.09.001

water and ice existing together in equilibrium below the normal bulk melting temperature, provided that the 'container' do not yield and that no special interaction between the pore walls and the ice and water is present. Fully saturated concrete cannot withstand the high pressures predicted by Clapeyron equation, meaning that the reason for water and ice coexisting at freezing and thawing has other explanations than those obtained by constrained pressures alone. It should be carefully noted that microscopic mechanical behaviour may give other results than the acroscopic hypothesis described above.

In real situations the concrete seldom becomes totally saturated, especially the entrained air voids are of dimensions making them practically inaccessible for water. Assuming that formed ice can 'grow' in the pore structure of the material in a stress-free manner, the limit saturation degrees will be 0.917 above this value, there is no space left for growth and the ice and water will start to assert a pressure to the pore walls. The limit 0.917 is based on the volume of ice being 9% larger than water. It has been experimentally proven that damage to concrete occurs at much lower saturation degrees than predicted theoretically for stress-free growth for partly saturated situations, e.g. see the results presented in [5].

Due to implications of both the close container and hydraulic pressure theory, yet another mechanism for the action of frost damages in concrete has been proposed. This mechanism is initially based on the observations on frost-induced heaving in soils. From experiments it was observed that in the cold end of a unidirectionally cooled cylindrical soil specimen, ice lenses were able to grow by consuming water from the warmer parts of the specimen and that the resulting ice lenses were able to assert considerable pressures, [6]. Observing length changes of samples during times of a constant freeze temperature, it was suspected that also ice lenses in concrete may attract surrounding water in a way similar to that of frost-induced heaving in soils, but in this case in a microscopic perspective only. The mechanism, introduced in [7], was referred to as the osmotic micro ice body growth. According to the hypothesis, freezing is initiated in some of the larger pores when cooling proceeds, the unfrozen water in the smaller pores will have a tendency to be transported from the smaller pores into the large ones where it will freeze onto the existing ice bodies. The transient character of transport of water to the ice bodies is, according to the hypothesis, the explanation for experimentally observed expansions at constant temperature. An extended version of this hypothesis, also considering cases of salt-frost scaling, is presented in [8]. It is concluded to be difficult to verify the osmotic micro ice body growth hypothesis experimentally; this is, partly, due to that the governing processes occur at the microscopic level. Some interesting discussions on the applicability of the hypothesis are performed in [9,10].

Besides, the three main mechanisms discussed to this end it has been proposed that super saturated water and ice in a porous material, assumed water and ice having their respective bulk phase properties, should be separated by a meniscus surface being submitted to a surface energy [11]. For such cases the meniscus radius or equally the hydraulic radius can be related to the temperature of fusion. Measurements on Vycor glass have been performed, indicating the value of the surface tension in the ice–water interface [12]. In this context, relevant information is also to be found in [13].

By using the surface tension in the curved ice–water interface and adopt it as a true material parameter, it is possible to evaluate the pore size distribution by using suitable additional assumptions together with measurements on the ice contents at different temperatures, e.g. see [14]. However, the measured hysteresis in ice content between freezing and thawing situations raises a number of questions regarding the relevance of the method. It can be argued that the development of the shape of ice bodies is markedly different during freezing and thawing, which should result in different active surface areas for these cases. The interpretation of the hysteresis in freezing curves during heating and cooling is discussed in [12].

Here the relation between measured length changes during freezing and thawing is compared to ice contents at corresponding temperatures using three different concrete qualities. Experimental results of this kind can be used to partly verify different hypotheses for ice growth and its damaging effect. Performing experiments directly devoted to verifying the discussed existing ice growth hypothesis are concluded to be very difficult and fall outside the scope of this work.

Each concrete quality, in this investigation, has been produced with three nominal contents of entrained air, 2%, 4% and 6%. The samples are conditioned to two different saturation levels, totally vacuum saturated and a saturation obtained by simple storage in water at normal pressures. The samples are analyzed for their ice contents during freezing and thawing using a scanning calorimetric technique, with a novel method to evaluate the raw data from the instrument, [15, 16]. The damage after and before exposure to freeze–thaw cycles is identified by using a non-destructive sonic measurement technique. Furthermore, length changes of samples are measured during the freeze/thaw cycles adopted. Methods have been presented on separate measurements of the kind used here or measurements of the length changes of samples when placed in a calorimetric instrument for the simultaneous registration of ice growth, e.g. see [10,17–19]. Besides the above-mentioned measurements, a picture analyze method was used on thin sections of the different concrete qualities. This method gives both the total air 'bubble' content and the size distribution of the same 'bubbles' in the material.

The results from the investigation show the importance of the air bubble content in concrete and the saturation degree of the tested samples. By studying the obtained ice content curves at freezing and thawing for the different samples and saturation degrees together with the comparison with their corresponding length changes, the overall performances of the different concretes can be obtained. Further, from the results presented, important information needed for the verification of different proposed mechanisms describing frost damages is provided.

Besides the quantitative examination of the different main hypothesis for the action of freeze and thaw induced damages based on different experimental results, the present paper also demonstrates the difficulties in accurately calculating the amount of ice formed at different freezing and thawing temperatures from considering data from the calorimetric approach. With the purpose to find a more exact method, the assumption of the calorimetric approach is described in detail and suggestions on complimenting experiments and general improvements are also discussed.

Accepting some inaccuracies in the determination of the ice amounts in the samples at the freezing and thawing situations studied, the presented results are ideally suited for the verification of mechanical models aiming at constituting the relation of ice concentrations in the pores of a material to the developed strains and stresses. Such analysis is, however, outside the scope of the presented investigation.

A special calorimetric test involving measurements down to about −145 °C has been included in this investigation. Using the proposed method for calculating the ice contents at different temperatures based on the calorimetric raw data, it was concluded that no ice was formed below about −50 °C.

2. Concrete recipes and preparation of samples

Nine different recipes were prepared for the investigation. Three different, water-to-cement ratio, concrete types were

produced, each with three different nominal 'target' air contents of 2%, 4% and 6%. The w/c = 0.6 concrete with air contents 2%, 4% and 6% were produced with 340, 350 and 335 kg/m^3 cement, respectively. The corresponding values for the 0.5 and 0.4 water-to-cement ratios in use were 475, 480 and 480 kg/m^3 (w/c = 0.5) and 515, 525 and 525 kg/m^3 (w/c = 0.4).

The samples were produced in 120-l batches in the laboratory. Two different granite aggregates were used, 0–3 mm and 4–8 mm. Approximately equal mass amounts of the two fractions were used for all different mixes. A portion of the aggregate in use was dried in an oven the day before the manufacture of the samples, in order to be able to adjust recipes for water on the surfaces of the sand and stones. The oven dried aggregates were never used to produce the samples, but only to check the actual moisture content. The water-to-cement ratios presented in this work are related to the total water and not to the SSD condition.

The two fractions of aggregates were mixed with cement before adding water. A Swedish sulphate resistant Portland cement was used (anläggningscement). In the case where the nominal air content was set to 4% or 6% an air-entraining agent was used. The water content in the agent was compensated for in order to get the correct target water-to-cement ratio of the mix.

The concrete was placed in two moulds with sides 0.2 × 0.5 × 0.5 m and in cubic moulds with sides 0.1 m. The moulds filled with concrete were vibrated a few seconds before covering them with plastic to prevent evaporation. About 5 l of the mixes where used to measure the density and air content of the fresh concrete. The fresh concrete workability was also tested using a simple slump test.

After one day of curing at sealed conditions, the concrete was sawn into small cylinders with diameter 1.4 cm and length 6.0 cm. The samples were produced to fit the calorimetric device adopted in this investigation. By direct ocular investigations it was concluded that no damage of samples was introduced by the early treatment. However, no mechanical strength measurements were performed to verify this fact more rigorously.

Prisms with dimensions 2 × 2 × 16 cm suited for length change measurements during freezing and thawing and sonic E-modulus measurements were produced, and plates with sides 10 × 10 × 5 cm were sawn out from blocks. The latter sets of samples are suited for the evaluation of air content of hardened concrete and the spacing between air voids.

Due to the cylinders being core-drilled to a diameter of 1.4 cm, which is small compared to the aggregate size (up to 8 mm), the ITZ is highly likely to percolate through the sample, e.g. see [19]. This might reduce the hydraulic pressure generated by freezing, which is noted to be a drawback of the method. The choice of the sample size was based on the limited space in the calorimetric device. No direct measurement concerning the influence of the ITZ on the freeze–thaw behaviour was performed in this study.

Half of the produced samples of different dimensions and qualities were stored submerged in water in about four months before testing. The other half of samples were dried and vacuum saturated in order to obtain total water saturation in the pores. From this procedure, the total porosity of samples was, also, evaluated by gravimetric measurement of samples by measuring the weight of saturated samples both in air and submerged in water.

3. Calorimetric measurements

The micro-concrete cylinders with diameter 1.4 cm and length 6.0 cm were used in the calorimetric tests. A Calvet-type scanning calorimeter (SETARAM) operating and calibrated to work between about 20 and −130 °C was used.

The temperature scanning consisted in the normal case of a cycle starting at 20 °C and going down to −80 °C and then back to 20 °C again. The freeze–thaw rate was set to 0.09 °C per min, making the total cycle last about one and a half day.

Fig. 1. Top of the SETARAM scanning calorimeter showing the liquid nitrogen supply tube and the reference and sample container.

The cooling system consists of liquid nitrogen which flows through the outer shell of the calorimetric vessel. The outer part of the calorimeter consists of a wall construction which is evacuated to vacuum to prevent heat exchange with the environment. The reference and sample containers are located at top of the calorimeter, see Fig. 1. The air in reference and sample containers is evacuated to a state of vacuum and then filled with dry nitrogen gas at atmospheric pressure before testing. The instrument is carefully calibrated for this condition in the chambers.

The size of samples is chosen so as to fit the sample containers as tightly as possible. The gap between sample and inner sample holder wall is approximately 0.5 mm. By evaluating data from measurements, this gap was shown to delay the heating and cooling very little. It is, however, very difficult to prevent water from being expelled from the sample caused by ice formation. This may contribute to water being adsorbed on the inner sides of the chamber walls, which will affect the heat response measurement in an unwanted manner. It has been suggested to wrap up the sample with, for example, aluminum foil to prevent condensation of water on chamber walls. It can be expected, however, that it is very difficult to prevent water to be expelled from the micro-structure of the sample, even when using such methods.

A totally dried reference concrete sample, of the same dimensions as the tested samples, is used in the reference chamber. The same reference is used throughout all tests in this investigation. This type of reference sample simplifies the calibration of the measurements compared to the use of other materials such as aluminum.

While in use, the instrument records the calibrated heat supplied to or released from the specimen, that is, the calorimeter measures the difference in the response of reference and the sample vessel. At the same time, the corresponding actual temperature in the sample chamber is recorded.

The sample is weighed before and after measurements. Typically the loss of water from the sample is about 0.1 wt.% of the total initial amount of water in the sample. Before testing, the samples were stored in water for about 4 months, and half of these samples were also vacuum saturated to obtain total saturation of pores in the material.

4. Evaluation of calorimetric measurement results

The measured results, see Fig. 2 (left), are evaluated in the sense that the integral values of the heat response curve are calculated, see solid line in Fig. 2 (right). The integrated heat response gives two curves representing the relative accumulated heat during

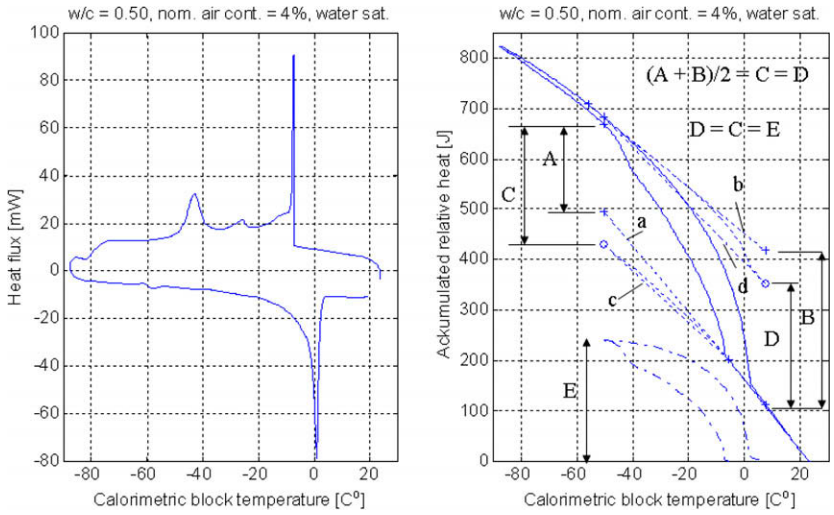

Fig. 2. Measured output data from calorimetric device (left) and integrated values of the heat response (right, solid line) and data treatment to achieve a proper baseline correction (right). The sample with w/c = 0.5 and the nominal air content of 4%, is investigated.

freezing and thawing, respectively. These functions are used explicitly to estimate the changes in the heat capacity of the sample during the test. It should be noted that information from this type of measurement is lacking making it impossible to make such corrections of heat capacity in an exact manner.

The heat capacity of the sample changes due to ice and solid matrix having different properties in this respect and that ice is formed continuously during the experiment. Besides these heat phenomena, an important portion of the measured heat is, due to the latent energy, required to form ice (or to melt ice).

The challenge of evaluating the data in a stringent way concerns the prediction of how much heat goes into changing the temperature of the sample (with different amounts of ice in it) and how much goes into forming ice (or melting ice). Two baselines are constructed by making assumptions of the integrated accumulated heat of water and ice separately. Weighted values between these curves are calculated and their magnitudes are dependent on how much is (assumed) formed at different temperatures, see Fig. 2 (left).

The difficulty of compensating the raw data from the calorimeter for the effect of the dependence of fusion energy on temperature is realized. In [20] a explicit temperature dependence expression is used, however, in the method adopted here, it is difficult to separate the baseline correction itself with any correction for changes in fusion energies. Due to this, one is forced to accept the inaccuracies which this direct method may cause, until a separate complementing measuring technique can be realized. The method, further, utilizes the important property that the total accumulated heat must go back to its initial value after a completed cycle.

The detailed description of how to calculate the amount of ice formed at different freezing and thawing temperatures is as follows. The first step concerns the extrapolation of the initial total heat capacity of the system valid before freezing, see the curve denoted by *a* in Fig. 2 (right). In the same manner the extrapolated heat capacity, valid for the case when all ice has been formed, can be constructed, see the curve denoted by *d* in Fig. 2 (left). The energy jump denoted by *A* in Fig. 2 (right) is the heat difference between the extrapolated fictive energy level, given by the *a* curve, and the true measured total accumulated energy level at the end of the active ice forming stage. The energy jump *A* is smaller than the real energy jump caused by the fusion energy involving formation of ice, since ice is continuously formed during the freezing process not accounted for in the extrapolated baseline curve of *a*. In the same manner, the energy jump from the frozen stage to the stage when all ice is melted given by *B* in Fig. 2 (left), overestimates the total fusion energy due to melting.

According to the method of extrapolation, the real total required energy to convert all water to ice or vice verse must lie somewhere in between the values of *A* and *B*. In the method adopted, the explicit and somewhat crude assumption that the total required energy to convert all water to ice or vice verse of the sample is the mean value of *A* and *B*, i.e., $(A + B)/2$ is adopted. The choice of this direct assumption is a consequence of the experimental procedure, which is lacking information making an 'exact' calculation impossible as discussed before. In [10] the described assumptions was checked for its performance by running a calorimeter test from room temperature to about $-20\,C^o$ using pure water. The test gave as a result a deviation of about 2% of the tabulated heat of fusion of ice, which indicates that the adopted direct method, in fact, performs in a manner acceptable for the purposes in this investigation. The obtained shape of the freezing and thawing curve is believed to be calculated with quite good accuracy. Naturally, the dependency of the heat capacities of water, ice and the solid and the heat of fusion itself on the temperature, contributes to making exact calculations difficult.

The mean value of the energy jumps $C = D$ defined by *A* and *B*, see Fig. 2 (right), is used to define new endpoints (marked with circles in Fig. 2 (left)) of the curves denoted by *c* and *d*. The next step in the procedure consists of making a non-linear weighting between the extreme curves *a* and *c* during the freezing process and between the extreme curves *b* and *d* during the thawing process, see Fig. 2 (right). The two obtained weighted curves, i.e., the ones lying in between the curves *a* and *c* and in between *b* and *d*, are used as the baselines of the experiment from which the accumulated energy related to the ice formation can be evaluated. In the lower part of Fig. 2 (right) the 'extracted' energy accumulated in the ice phase is shown.

5. Measurements of length changes during freeze/thaw tests

Four months old water saturated and vacuum saturated samples of dimensions $2 \times 2 \times 16$ cm were tested for the length changes when exposed to a single freeze–thaw cycle of the same type used in the calorimetric tests. The device shown in Fig. 3 was used. This device was placed in a chamber where the temperature could be controlled.

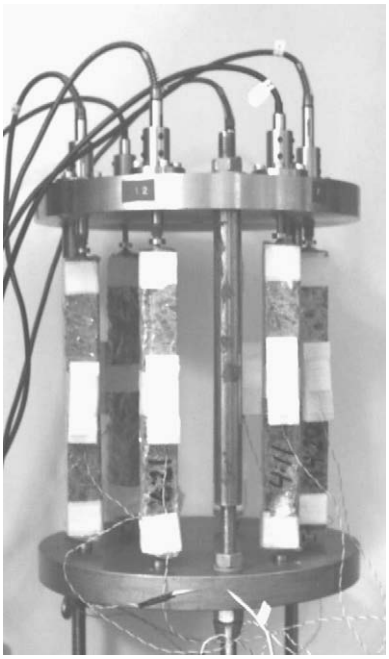

Fig. 3. Sample holder with six concrete prisms for the length change measurements during freezing and thawing. The LVDT sensors are placed at the top of the samples. Samples are covered with a thin flexible plastic foil to avoid evaporation during test.

Before testing, the samples were supplied with a small metal cone glued at the top and bottom of the specimen. This cone is constructed to perfectly join the gauge on the sample holder which can contain maximum six samples. This construction is used to avoid slipping and formation of small ice crystals on supports. The use of the metal cone and the matching gauge at both sides of the samples made it possible to eliminate measured length changes other than those developed in the sample itself.

Before mounting the samples on the holder they are wrapped in plastic foil to prevent evaporation from the samples. Samples are also supplied with a thermo-element which records the temperature on the specimen surface independently of the surface temperatures of other samples in the test. The displacement of samples is recorded by LVDT-sensors which are connected to a data logger and a computer. The specimen holder consists of an invar construction which minimizes changes in the dimension of the holder during the test at different temperatures.

The sample holder armed with the samples is placed in a large refrigerator which automatically runs a desired temperature cycle. Due to limitations in the performance of the LVDT-sensors at low temperatures, the minimum temperature in use in test was −55 °C. The cycle adopted was 20 to −55 °C and back to 20 °C with a cooling and heating rate of 0.09 °C per min, making a whole cycle last about one day.

The specimen was weighed before and after measurements to check the loss of water from the sample during the test. Typically, a loss of 0.6% of total initial water was observed.

Results of the length change measurements are, in accordance with the ultra-sonic measurements, detecting cracks in sample caused by a freeze/thaw cycle. That is, a large remaining measured deformation after a complete freeze/thaw cycle of a sample was also registered by measuring the loss in the E-modulus on the same sample, using the adopted ultra-sonic technique. Furthermore, the deformation during freezing and thawing is in accordance with the evaluated ice contents from the calorimetric measurements, e.g., when the ice content decreases according to the calorimetric measurements, the length change decreases in a similar fashion. This is especially true for vacuum saturated samples and water saturated samples with low air contents.

6. Detection of damage using an ultra-sonic technique

Concrete samples with the dimensions $2 \times 2 \times 16$ cm were tested for loss in sonic elastic-modulus due to experiencing basically the same type of a freeze–thaw cycle used in the calorimetric tests. The samples used in the length change experiments where analyzed before and after this exposure freezing and thawing cycles using a GRINDOSONIC instrument, see Fig. 4.

The GrindoSonic instrument records a vibration induced by a light mechanical impulse, makes an analysis in the time domain and measures the natural frequency of the dominant vibration mode against a precision reference oscillator. The natural frequency of the dominant vibration mode is very much dependent on the presence of cracks of other types of defects leading to a decrease in the E-modulus of the material in the test. The non-normalized value of the E-modulus in an elastic material is approximately proportional to the square of the natural frequency in the same material. It is therefore ideally suited for determination of the degree of damage of specimens when one wishes to adopt non-destructive methods.

7. Measurements of air pore-system of hardened concrete

Obtaining an air void pore system with certain qualities is central for a frost durable concrete, e.g. see [2,21]. For this purpose it is important to analyze it by experiments. Concrete samples with the dimensions $10 \times 10 \times 5$ cm were tested for air content and the 'mean' spacing between air voids using an image technique. Sample surfaces (on the 10×10 side) were ground in a way so that a flat polished surface was obtained. Small cavities or other traces introduced by the surface grinding procedure were avoided as much as possible as it affects the measurement results. The wet surface ground samples were then supplied with a heated white coloured zinc-based paste over the surface and smoothly smeared on the surface using a plate with sharp edges. The paste fills the

Fig. 4. Equipment for evaluating the sonic E-modulus of concrete prisms (GRINDOSONIC). The concrete sample is placed on a soft plate. The instrument measures the vibration frequency when tilted with a small hammer (shown in the lower right hand-side of picture).

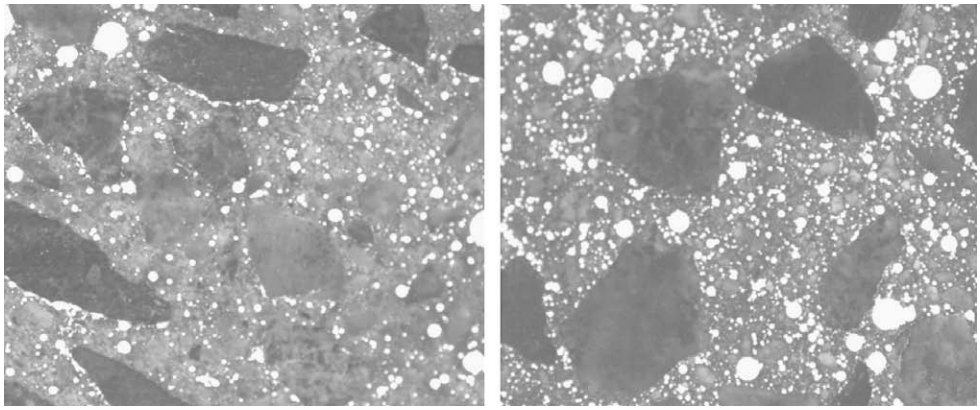

Fig. 5. Picture from LABEYE measurements. Example of the geometry of air pore system in a w/c = 0.60 concrete, left hand side shows a sample of air content 4.6% and right hand-side, an air content of 8.4%. Original size of pictures is 24 × 16 mm.

naturally present or entrained air voids and cavities on the surface and becomes visible due to its sharp white colours, see Fig. 5. The smallest observable 'bubble' size is in the range of 10–20 μm, which approximately defines the air bubbles to be between about 15 and about 1500 μm in diameter. Air voids in the hardened concrete of larger diameter size than 1500 μm are often considered as defects rather than playing an important role in describing the air 'bubble' volume and the size distribution.

There are certainly many air voids smaller than 10 μm and they can be influential. In [22] it is argued that the smaller voids fill relatively rapidly with water, so they can contribute to the "closed container" damage. In this investigation, however, such small air voids is not included in the analyses leading to the air content and the air void spacing factor of the samples.

The method is based on using a microscope to magnify different regions on the polished surface using the LABEYE equipment. The visible air 'bubble' diameters on the surface are only equal to the real diameters if the surface cuts the bubbles in the centre. Naturally, this is only occurring with a certain probability for each observed bubble. The expressions for these probabilities are based on different size classes being defined. For example, the largest introduced size class is observed with the probability equal to 1 if the bubble size on the cut surface is measured to be in the largest introduced class interval. Further, measured bubble diameters on the cut surface being in the range of the smallest introduced size interval can with predefined probabilities belong to any of the introduced size classes. Using the above described method, the volume of different air bubble sizes (defined by the introduced size intervals in use) can be calculated. This was done in the current investigation but its results are not presented here. Naturally, the sum of these class size volumes constitutes the total air content of the hardened concrete examined.

By assuming a case of a mean air bubble size homogeneously distributed within the cement paste volume in concrete, the so-called Power's spacing factor can be calculated from the knowledge of the total air content and the air bubbles corresponding specific surface area. The values of this property are calculated from the output results from the LABEYE analysis presented and are shown in Tables 1–3 for the nine different concrete qualities studied.

It should be observed that the model only includes the existence of perfectly spherical bubbles and that any deviation from this will affect the results. Another important topic is that the model can yield negative values of volumes of different bubble sizes. Presumably, this is due to defining too many class intervals, which increases the risk of not adding any information to some of the classes. Another fact is that a lot of data must be collected to make the method valid. Furthermore, there is a built in human factor as the domains investigated cannot be chosen and investigated totally independently.

Table 1
Data for the concrete with the water-to-cement ratio 0.60 with the three nominal air contents 2%, 4% and 6%. The notations MC 602, MC 604 and MC 606 are used for the micro concretes tested.

	MC 602	MC 604	MC 606
Measured density of fresh concrete (kg/m^3)	2352	2269	2185
Computed density from mixing recipe (kg/m^3)	2294	2239	2169
Computed density using vacuum tests (kg/m^3)	2218	2140	2066
Measured air content of fresh concrete (–)	2.6	4.7	7.8
Measured air content using picture analysis (–)	3.2	4.6	8.4
Powers spacing factor using picture analysis (mm)	0.40	0.20	0.13
Porosity using vacuum tests (–)	0.181	0.203	0.232
Slump of fresh concrete (mm)	31	210	130
Approx. saturation degree (water saturated)	0.91	0.88	0.68
E-modulus ratio, before/after freezing, water saturated	0.78	0.98	1.01
E-modulus ratio, before/after freezing, vacuum saturated	0.31	0.64	0.91

Table 2
Data for the concrete with the water-to-cement ratio 0.50 with the three nominal air contents 2%, 4% and 6%. The notations MC 502, MC 504 and MC 506 are used for the micro concretes tested.

	MC 502	MC 504	MC 506
Measured density of fresh concrete (kg/m^3)	2357	2294	2271
Computed density from mixing recipe (kg/m^3)	2275	2233	2186
Computed density using vacuum tests (kg/m^3)	2222	2184	2109
Measured air content of fresh concrete (–)	2.0	3.6	5.4
Measured air content using picture analysis (–)	2.1	3.1	4.9
Powers spacing factor using picture analysis (mm)	0.54	0.24	0.15
Porosity using vacuum tests (–)	0.175	0.186	0.216
Slump of fresh concrete (mm)	140	140	110
Approx. saturation degree (water saturated)	0.92	0.91	0.78
E-modulus ratio, before/after freezing, water saturated	0.73	0.96	0.97
E-modulus ratio, before/after freezing, vacuum saturated	0.55	0.35	0.27

The exact and detailed description of the method for evaluating void size distribution, using a statistical basis as discussed here, can be studied in [23].

Results presented in [24] indicate the effect of surface structure of entrained air voids on the water movement during freezing and thawing. That is, not just air content and the spacing factor, but

Table 3
Data for the concrete with the water-to-cement ratio 0.40 with the three nominal air contents 2%, 4% and 6%. The notations MC 402, MC 404 and MC 406 are used for the micro concretes tested.

	MC 402	MC 404	MC 406
Measured density of fresh concrete (kg/m^3)	2357	2372	2280
Computed density from mixing recipe (kg/m^3)	2326	2274	2216
Computed density using vacuum tests (kg/m^3)	2244	2245	2211
Measured air content of fresh concrete (–)	2.5	4.2	6.1
Measured air content using picture analysis (–)	2.7	4.3	4.9
Powers spacing factor using picture analysis (mm)	0.54	0.34	0.16
Porosity using vacuum tests (–)	0.165	0.168	0.181
Slump of fresh concrete (mm)	10	32	75
Approx. saturation degree (water saturated)	0.86	0.93	0.81
E-modulus ratio, before/after freezing, water saturated	0.92	1.00	1.05
E-modulus ratio, before/after freezing, vacuum saturated	0.56	0.43	0.60

also morphology of the shells forming the air voids is thought to influence the performance of cement based materials during freezing and thawing. Different morphology of entrained air voids can be generated using different anionic surfactants. Surface structure effects on the freeze/thaw behaviour cannot be studied by the LABEYE equipment method discussed here, therefore other methods have to be used for investigations of this case.

8. Measurement results

The measurement results of this investigation are mainly the ice contents and the corresponding length changes obtained during a freeze–thaw cycle. The mechanical damage induced by this treatment is reported by measuring results involving the ultra-sonic method using the GRINDOSONIC instrument. Further, the air contents on fresh and hardened concrete are presented as well as the total porosities and Power's spacing factors.

The mass fraction of formed ice in relation to the mass of total water in the sample, for different temperatures on samples being water saturated, is shown in Fig. 6. The corresponding length changes, for the water saturated samples, are shown in Fig. 8. The corresponding situations for the vacuum saturated preparation procedure are illustrated in Figs. 7 and 9.

The independent measurements of Figs. 8 and 9, shown by solid and dashed lines, illustrate, in some cases, poor reproducibility. This might be due to bursting of water saturated air voids, which is not a strictly reproducible phenomenon.

The degradation in the E-modulus due to the freeze thawing process is presented in Tables 1–3. In these tables, results from the nine studied concrete qualities with the two different water preparations considered are shown. In these tables also the densities, porosities, air contents and Power's spacing factors are presented for all nine concrete qualities. The results of the E-modulus before and after freezing shown in Tables 1–3 are for one single complete freeze/thaw cycle, which is the same cycle used in the calorimetric and length change measurements.

As noted from the results on the E-modulus before and after freezing shown in Tables 1–3, two samples, in fact, obtained a slightly higher E-modulus after freezing as compared to the value measured before freezing. This is interpreted as a measurement inaccuracy effect rather than any real significant result.

The effect of the special case of two in a row repeated freeze/thaw cycles in terms of the calculated ice contents at different temperatures, obtained by using the raw data from the calorimetric device, is illustrated in Fig. 10. This type of investigation was only performed ones and is of importance when controlling the significance of the evaluation method, but also as an indicator on the rearrangement of water. That is, the change of appearance of water in different types of pore sizes and air voids.

A special calorimetric measurement concerns a situation where a special freeze–thaw cycle is adopted. In this a very low temperature is used, i.e., −145 °C. The purpose of the test is twofolded. First it was of interest to check if ice was formed between −55 °C

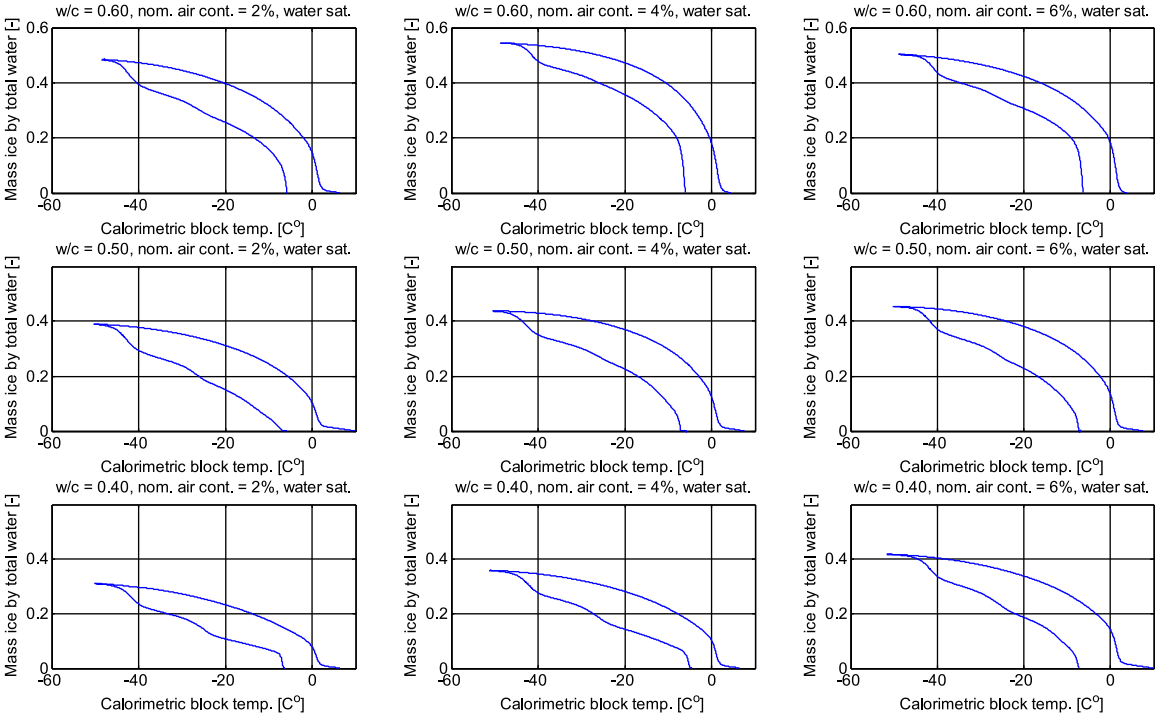

Fig. 6. Calculated amounts of ice formed at different temperatures using a baseline corrected method of the calorimetric heat flux data. Lower curves freezing and upper curves thawing. The results are for water saturated samples.

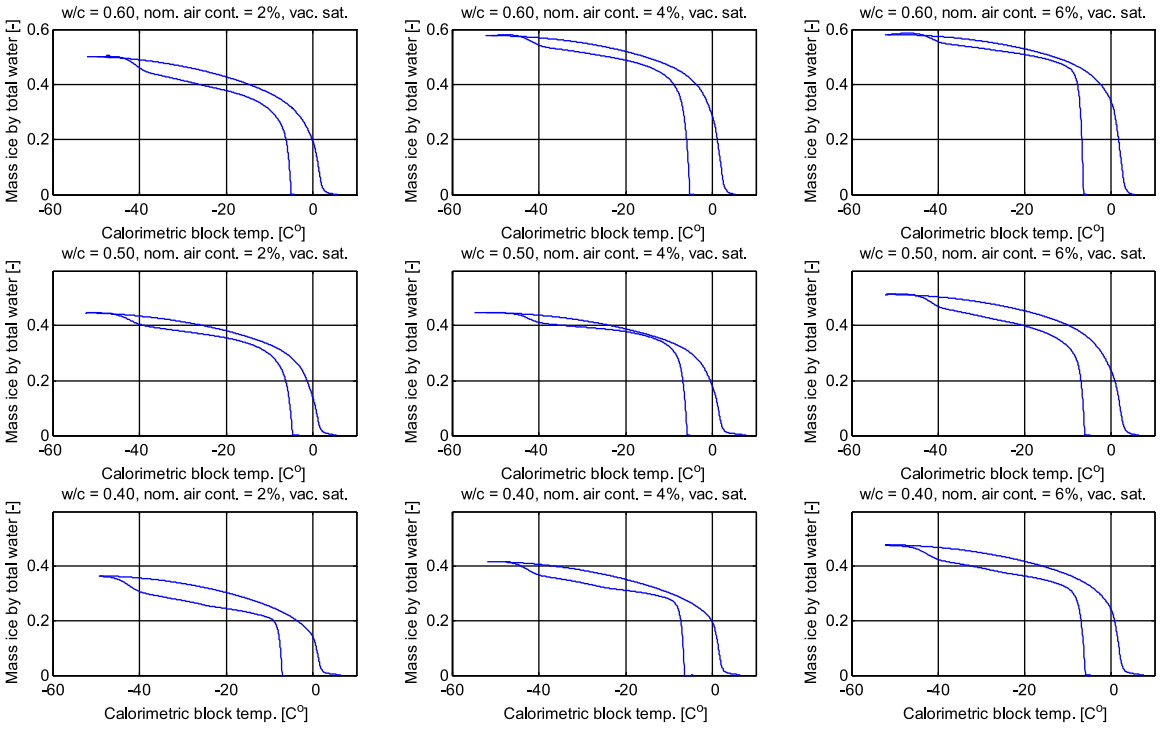

Fig. 7. Calculated amounts of ice formed at different temperatures using a baseline corrected method of the calorimetric heat flux data. Lower curves freezing and upper curves thawing. The results are for vacuum saturated samples.

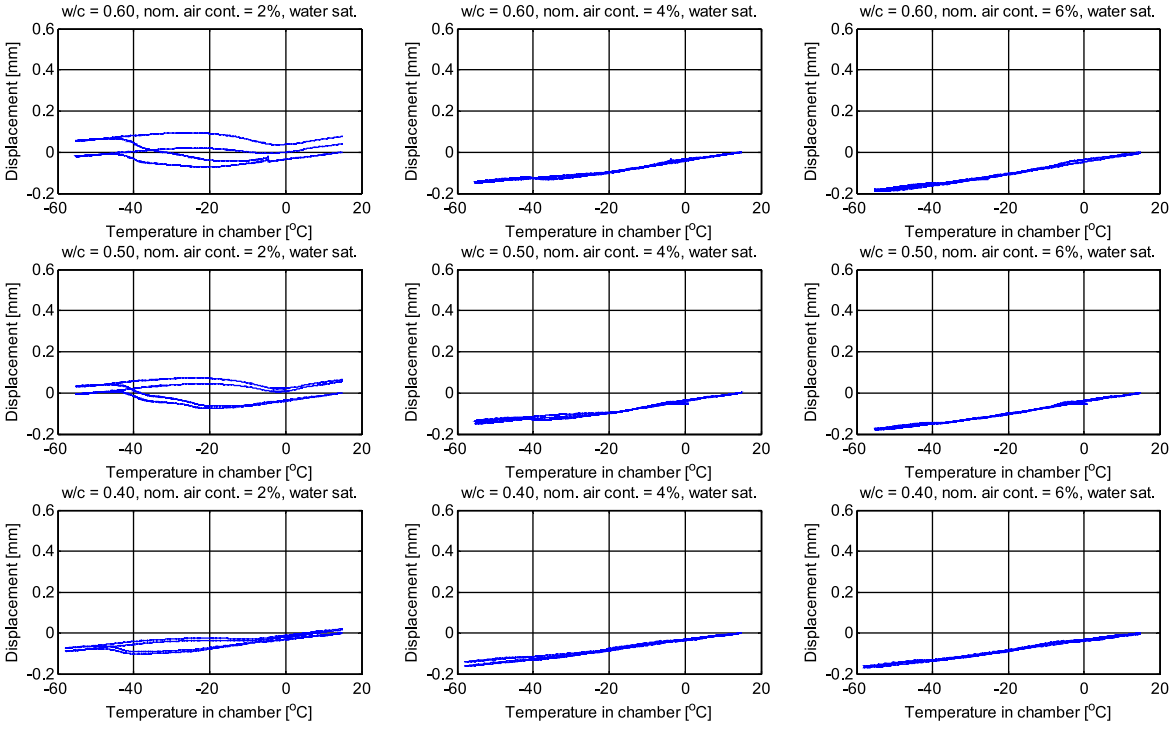

Fig. 8. Length change measurements of samples exposed to a cycle in temperature starting at room temperature and going down to about −60 °C and then back to room temperature again. The initial length of samples is 160 mm. Lower curves freezing and upper curves thawing. The results are for water saturated samples, two independent measurements are shown for each concrete quality.

and −145 °C , which is generally believed not to give rise to formation of ice. The second issue was to have a measure of the calorimetric performance beyond the manufacturers recommended and calibrated regions. The result from this test is shown in Fig. 11.

9. Discussion

The main purpose of this investigation was to demonstrate the relation between the measured length changes during freezing and

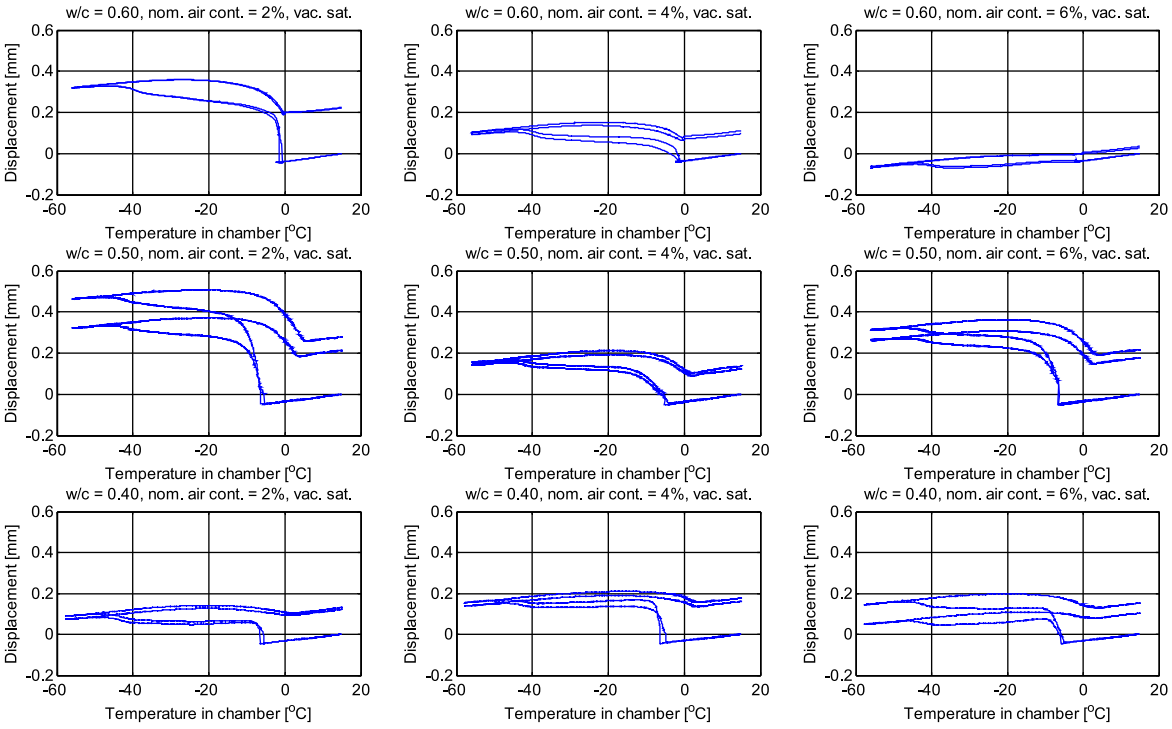

Fig. 9. Length change measurements of samples exposed to a cycle in temperature starting at room temperature and going down to about −60 °C and then back to room temperature again. The initial length of samples is 160 mm. Lower curves freezing and upper curves thawing. The results are for vacuum saturated samples, two independent measurements are shown for each concrete quality.

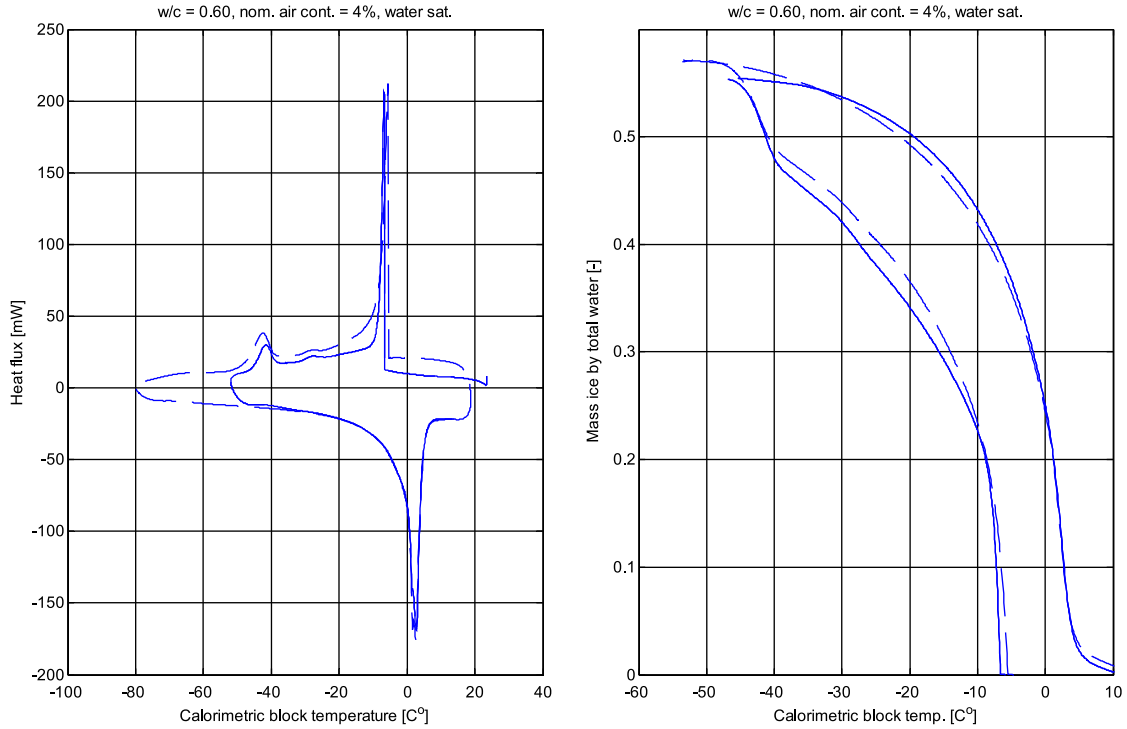

Fig. 10. Measured output data from the calorimetric device (left) for a case of two cycles (dashed line first cycle and solid line second cycle) and calculated ice contents at different freezing and thawing temperatures (dashed line first cycle and solid line second cycle).

thawing and the predicted amounts of ice in the samples at the corresponding temperatures. The results of this investigation show that the shape of the length change curves and the calculated ice amount curves for vacuum saturated samples are very similar, e.g., compare Figs. 7 and 9. This does, indeed, indicate that the method of evaluating the calorimetric data to obtain ice amounts at different freezing and thawing temperature is adequate. However, as pointed out earlier, experimental data, of this

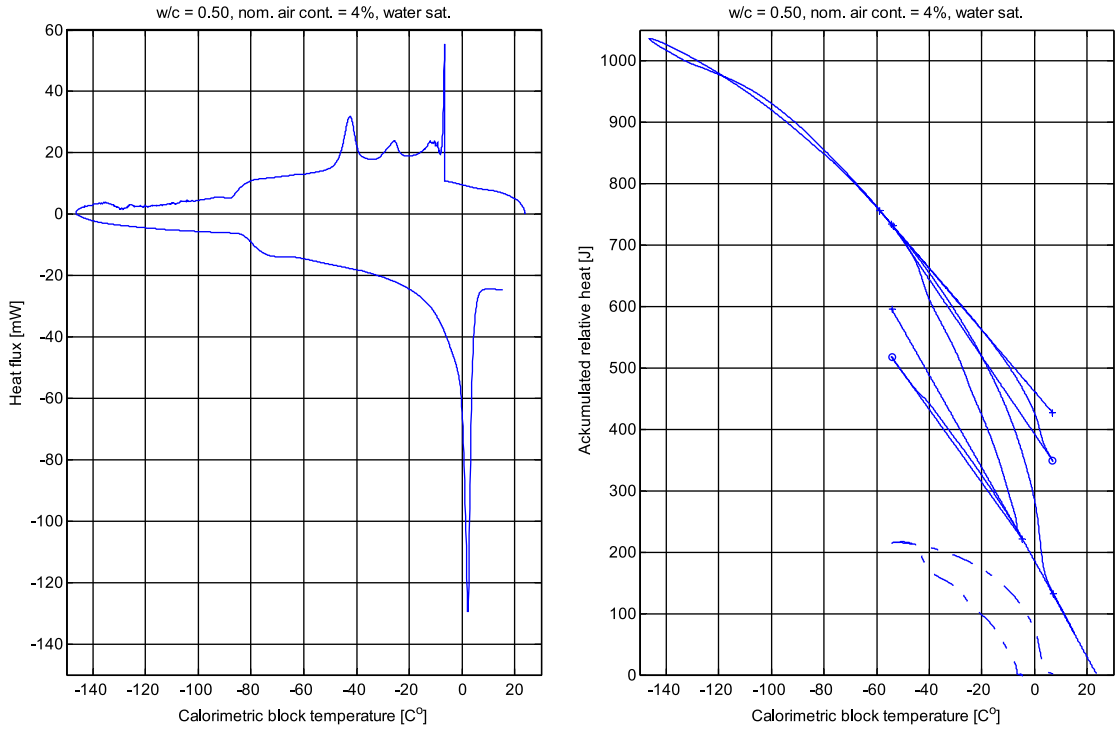

Fig. 11. Measured output data from calorimetric device (left) for a case consisting of going down to about −150 °C in temperature. Right-hand side of figure shows the corresponding integrated values of the heat response (solid line) and data treatment to achieve a proper base line correction, see also Fig. 2.

investigation, are missing making an 'exact' evaluation impossible. It is concluded that it is mainly the determination of the maximum ice amount which is difficult to predict. On the contrary the overall shape of the ice amount curves seems to be adequately computed by the suggested method.

The drawback of the uncertainties of the method of analyzing the calorimetric measurements for the absolute maximum ice amount may be eliminated by using some complementing experiments, based on for example, NMR or ultra-sonic measurements. Presumably, a complementing method should make it possible to make a better choice of baselines than the one used here.

Naturally, any macro mechanical understanding of the frost damage phenomena, studied here, demands the knowledge of the amount of ice present at different situations. By this reason the development of a robust method to calculate the ice content during freezing and thawing becomes very crucial whenever the development of continuum mechanical methods for frost induced damage is of interest. As is the case of, for example, moisture induced strains and stresses, the moisture distribution in the body of consideration must be determined. In fact state variables such as the moisture content and temperature are much more easily experimentally measured than compared to the concentration of ice in the porous material under consideration.

Here only completed freeze–thaw cycles were investigated, that is, the temperature cycle in the calorimeter was such that the temperature was sufficiently low to assure that all possible ice formation had taken place. In real situations, the cycles are dictated by the winter climate resulting in ice amount curves being significantly different from the total cycles investigated here. Therefore the current investigation must be complemented by measuring 'scanning' curves in the hysteresis domain between the extreme curves of freezing and thawing, whenever generalizations of this kind are of interest. The proposed method of evaluating the ice amounts is supposed to be ideally suited for such examinations.

It should be remarked that no direct correlation between the measured Powers spacing factors for the different samples and the general shape of the measured ice contents and length changes, at different temperatures, could be found in this investigation.

10. Conclusions

A novel method of evaluating the ice contents from measurements using a scanning calorimetric technique is presented. By performing separate measurements on the length changes on samples exposed to identical freeze/thaw cycles as the ones tested in the calorimeter, it is possible to make some conclusions concerning the relevance of different proposed mechanisms for the action of frost damages.

Further, it is concluded that the presented results on length changes contra ice amounts of samples of different qualities are ideally suited for verification of continuum mechanical models based on the same principles as, for example, truly thermo-elastic approaches.

Some of the most apparent and direct conclusions of this investigation include:

1. The air content must be higher than the natural content of 2% in order for water-saturated concrete samples to withstand the adopted freeze–thaw cycle adopted in this investigation. The use of a low water-to-cement (high strength) concrete did only improve the performance slightly for samples having about 2% in air content, e.g. compare with Fig. 8 and Tables 1–3.
2. Water saturated samples with nominal air contents of 4% and 6% show very little influence of the ice formed, since the unit length change was observed to be almost linearly related to a unit temperature change, as expected in normal temperature volumetric changes, see Fig. 8.
3. The water saturated samples with the nominal air content of 2% show a length change behaviour, during the freeze–thaw cycle, which is similar in shape to the calculated ice contents for cor-

responding temperatures. This indicates that strain in the sample, in this case, is linearly proportional to the ice content. Compare Figs. 6 and 8.

4. The vacuum saturated samples, having a water saturation degree close to one and a significant amount of water present in the air voids, could under no circumstances withstand the adopted freeze–thaw cycles. Both the degradation in terms of E-modulus and permanent displacement after freeze cycle prove this statement, i.e., compare Fig. 9 and results in Tables 1–3. Cases where concrete under natural conditions obtains such high saturation degrees must, however, be considered to be very rare.
5. A repeated freeze–thaw cycle resulted in the same ice content, at different freezing and thawing temperatures, in both considered cycles, e.g. see Fig. 10. This result strongly suggests that the rearrangement of the location of water in the different pore sizes occurs to a very little extent. If water, for example, was transported to the air voids during the first freeze/thaw cycle, a significantly different freezing process would be expected. This is due to the fact that water present in large pore freezes at a higher temperature than water present in the fine pores. The conclusion 5 is not necessarily valid, because the water movement could be reversible.
6. The low temperature test, the results of which are shown in Fig. 11, indicates that no ice is formed in the pore system of samples below about −55 °C. Indeed these low temperatures can be of interest in special applications such as the use of concrete for the storage of liquid petroleum gas.
7. The hysteresis in ice formation at freezing and thawing is less dominant for the vacuum saturated samples compared to the water saturated ones.

The presented results are restricted to the case of the freeze–thaw cycle adopted. For general cases, the ice formation hysteresis must also be studied by identifying the general 'scanning' behaviour in between the extreme curves describing ice formation at freezing and thawing for the complete freeze–thaw cycle investigated here. It is concluded that the proposed measurement and evaluation technique presented here can be straightforwardly extended to study such cases.

Acknowledgements

The Swedish organization SBUF (Svenska Byggbranchens Utvecklingsfond) and SKANSKA is kindly acknowledged for sponsoring parts of the presented research work.

References

[1] Powers TC. A working hypothesis for further studies of frost resistance. J Am Concr Inst 1945;16:245–72.
[2] Powers TC. The air requirement of frost resistant concrete. In: Proceedings, highway research board, No. 29. Bulletin 33; 1949.
[3] Vuorinen J. On the behaviour of hardened concrete during freezing. The State Institute for Technical Research, Finland, Publication 145; 1969.
[4] Fagerlund G. The international cooperative test of the critical degree of saturation method of assessing freeze/thaw resistance of concrete. Mater Struct 1977;10:56.
[5] Fagerlund G. Critical degrees of saturation at freezing of porous and brittle materials. Doctoral thesis, Division of building materials, Lund Institute of Technology, Report 34; 1972.
[6] Taber S. Mechanics of frost heaving. J Geol 1930;38:303–17.
[7] Powers TC, Helmuth RA. Theory of volume changes in hardened portland-cement paste during freezing. In: Proceedings, highway research board, No. 32. Bulletin 46; 1953.
[8] Setzer MJ. Development of the micro-ice-lens model, frost resistance of concrete. In: Setzer MJ, Auberg R, Keck H-J, editors. Proceedings. Canchan: RILEM Publications S.A.R.L; 2002.
[9] Lindmark S. Mechanisms of salt frost scaling of portland cement-bound materials – studies and hypothesis (Doctoral thesis). Division of Building Materials, Lund Institute of Technology, Report TVBM – 1017; 1998.
[10] Fridh K. Internal frost damage in concrete – experimental studies of destruction mechanisms (Doctoral thesis). Division of Building Materials, Lund Institute of Technology, Report TVBM – 1023; 2005.
[11] Helmuth RA. Dimensional changes of hardened portland cement pastes caused by temperature changes, Proceedings, Highway Research Board, No. 32. Bulletin 46; 1961.
[12] Brun M, Lallemand A, Quinson J-F, Eyraud C. A new method for simultaneous determination of the size and the shape of pores: the thermoporometry. Themochim Acta 1977;21:59–88.
[13] Defray R, Prigogine I, Bellemans A, Everett DH. Surface tensions and adsorption. New York: Wiley; 1966.
[14] Bager D, Sellevold E. Low temperature calorimetry as a pore structure probe. In: 7th International congress on the chemistry of cement, Paris; 1980.
[15] Johannesson B, Fagerlund G. Concrete for the storage of liquid petroleum gas – freeze/thaw phenomena and durability at freezing to −50 °C. Division of Building Materials, Lund Institute of Technology, Report TVBM – 7174; 2003.
[16] Fagerlund G, Johannesson B. Concrete for the storage of liquid petroleum gas, Part II – influence of very high moisture contents and extremely low temperatures, −196 °C. Division of Building Materials, Lund Institute of Technology, Report TVBM - 7185l; 2005.
[17] Valore RC. Volume changes in small concrete cylinders during freezing and thawing. J Am Concr Inst 1950;21:6.
[18] Verbeck G, Klieger P. Calorimeter – strain apparatus for study of freezing and thawing concrete. Highway Research Board, Bulletin 176; 1958.
[19] Hooton RD. What is needed in a permeability test for evaluation of concrete quality? In: Roberts LR, Skalny JP, editors. Pore structure and permeability of cementitious materials, vol. 137. Pittsburgh (PA): Materials Research Society; 1989. p. 141–9.
[20] Penttala V. Freezing-induced strains and pressures in wet porous materials and especially in concrete mortars. Concr Sci Eng 1998;7:8–19.
[21] Warris B. The influence of air entrainment on the frost resistance of concrete. In: Swedish cement and concrete research institute, proceedings No. 36; 1964.
[22] Fagerlund G. Predicting the service life of concrete exposed to frost action through a modelling of the water absorption process in the air-pore system. In: Jennings H, editor. The modelling of microstructure and its potential for studying transport properties and durability. Amsterdam: Kluwer; 1996. p. 507–37.
[23] Underwood EE. Quantitative stereology. Marietta (Georgia, USA): Lockheed-Georgia Company; 1970.
[24] Atahan HN, Carlos Jr C, Chae S, Monteiro PJM, Bastacky J. The morphology of entrained air voids in hardened cement paste generated with different anionic surfactants. Cem Concr Compos 2008;30(7):566–75.